Journal Pre-proof

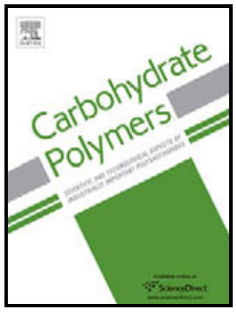

Retinoic acid grafted to hyaluronan for skin delivery: Synthesis, stability studies, and biological evaluation

Gloria Huerta Angeles, Martina Brandejsová, Petr Štěpán, Vojtěch Pavlík, Jana Starigazdová, Paulina Orzol, Kateřina Kopecká, Pavlína Halamková, Jaromir Kulhánek, Vladimir Velebný

PII: S0144-8617(19)31401-8

DOI: https://doi.org/10.1016/j.carbpol.2019.115733

Reference: CARP 115733

To appear in: *Carbohydrate Polymers*

Received Date: 17 October 2019

Revised Date: 19 November 2019

Accepted Date: 9 December 2019

Please cite this article as: Angeles GH, Brandejsová M, Štěpán P, Pavlík V, Starigazdová J, Orzol P, Kopecká K, Halamkovaacute, Kulhánek J, Velebný V, Retinoic acid grafted to hyaluronan for skin delivery: Synthesis, stability studies, and biological evaluation, *Carbohydrate Polymers* (2019), doi: https://doi.org/10.1016/j.carbpol.2019.115733

Retinoic acid grafted to hyaluronan for skin delivery: Synthesis, stability studies, and biological evaluation.

Gloria Huerta Angeles,[1]* Martina Brandejsová,[1] Petr Štěpán,[1] Vojtěch Pavlík,[1,2] Jana Starigazdová,[1] Paulina Orzol,[1] Kateřina Kopecká,[1] Pavlína Halamková,[1] Jaromir Kulhánek,[1] and Vladimir Velebný[1].

[1]*Contipro a.s., Dolni Dobrouč 401, 561 02 Dolni Dobrouč, Czech Republic.*

[2]*Department of Dermato-venereology, Third Faculty of Medicine, Charles University, Prague, Czech Republic.*

[*]Corresponding author: huerta-angeles@contipro.com

Telephone +420 465 519 573

Fax +420 465 524 098

Graphical Abstract

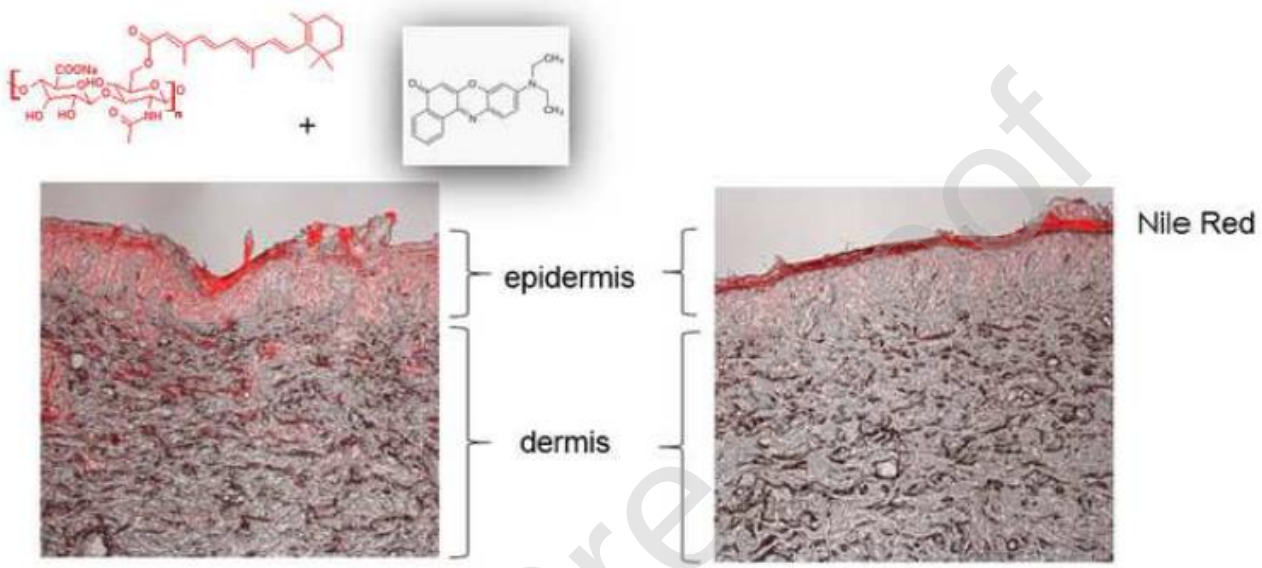

Highlights

- The stability of HA-ATRA is a function of the degree of substitution
- The use of morin increased the photostability of HA-ATRA
- HA-ATRA downregulates the proinflammatory cytokines IL-6 and IL-8
- HA-ATRA demonstrates ability to penetrate through epidermis and dermis
- The genomic activity of retinoic acid is kept after conjugation to HA

Abstract

All-trans retinoic acid (ATRA) was grafted to hyaluronan (HA) via esterification. The reaction was mediated by mixed anhydrides. A perfect control of the degree of substitution (0.5 to 7.5%) was obtained by varying the molar ratio of retinoic acid in the feed. The degree of substitution plays a significant role in the long-term stability. The photodegradation of HA-ATRA upon UVA irradiation resulted in β-ionone, β-cyclocitral and 5,6-epoxy-(E)-retinoic acid. The photostability of the conjugate had increased with the combination with morin. The chemical structure of HA-ATRA and its degradation products was elucidated using NMR spectroscopy, SEC-MALLS, and gas chromatography–mass spectrometry (GC-MS). ATRA did not loss its biological activity after conjugation, as demonstrated by gene expression. The derivative was able to penetrate across the stratum corneum. Besides, HA-ATRA downregulated the expression of anti-inflammatory interleukins 6 and 8. HA-ATRA would be expected to be used for transdermal drug delivery or cosmetics.

Keywords: Retinoids, skin, antioxidants, hyaluronan.

Chemical compounds studied in this work

Hyaluronic acid (PubChem CID: 24728612)

2-Ethylhexyl 2-cyano-3,3-diphenylacrylate (PubChem CID: 22571)

2-Ethylhexyl 4-methoxycinnamate (PubChem CID: 21630)

(±)-6-Hydroxy-2,5,7,8-tetramethylchromane-2-carboxylic acid (Trolox; PubChem CID: 40634)

Avobenzone (1-(4-Methoxyphenyl)-3-(4-tert-butylphenyl)-1,3-propanedione; CID: 51040)

Butylated hydroxyanisole (BHA; PubChem CID: 517036)

Butylated hydroxytoluene (BHT; PubChem CID: 31404)

Morin hydrate (2′,3,4′,5,7-Pentahydroxyflavone; PubChem CID: 16219651)

Retinoic acid (PubChem CID: 444795)

Retinyl palmitate (PubChem CID: 5280531)

Abbreviation list

ATRA all-*trans*-retinoic acid

Bc Benzoyl chloride

BHA Butylated hydroxyanisole

BHT Butylated hydroxytoluene

DCC *N,N´*-dicyclohexylcarbadiimide

DMAP 4-(Dimethylamino)pyridine

DMEM Dulbecco´s modified Eagles medium

DS Degree of substitution

EDC 1-ethyl-3-(3-dimethylaminopropyl) carbodiimide

FBS Fetal bovine serum

GlcA D-glucuronic acid

GlcNAc *N*-acetyl-D-glucosamine

HA Hyaluronic acid

HA-ATRA sodium retinoyl hyaluronate conjugate.

HaCaT Human keratinocytes

IL-1α Interleukin-1α

IL-1β Interleukin-1β

IL-6 Interleukin-6

IL-8 Interleukin-8

IL-12 Interleukin-12

IPA Isopropanol

MTT 3-(4,5-dimethylthiazol-2-yl)-2,5-phenyltetrazolium bromide

Mw Molecular weight

NHS *N*-hydroxysuccinimide

NR Nile Red

OMC 2-ethylhexyl 4-methoxycinnamate

RARE Retinoic acid response element

RH relative humidity

RMA Reactive mixed anhydride

RP Retinyl palmitate

RPL13A Ribosomal protein L13a

RT-qPCR Real-time quantitative reverse transcription

SD Standard deviation

TBA Tetrabutylammonium salt

TEA Triethylamine

TGA Thermal gravimetric analysis

THF Tetrahydrofurane

1. Introduction

Topical drug delivery is a route of administration on the skin and continuous delivered into the body through the skin (Xie, Ji, Xue, Ma, & Hu, 2018). Despite several advantages, the bioavailability of transdermal drug delivery systems is still low, because not all the drugs can easily permeate through the stratum corneum (Son, Lim, Kang, Jung, & Lim, 2017). Thus, topical delivery of molecules into the human skin is one of the main issues in dermatology and cosmetology (Essendoubi et al., 2016).

The retinoid family comprises vitamin A (retinol) and its natural derivatives such as retinal, retinoic acid and retinyl esters, as well as many synthetic analogs. All-trans-retinoic acid (ATRA) is one of the less efficient compounds applied topically. ATRA has been shown to improve clinical features of aging by reduction of wrinkles (Zhang & Duan, 2018), improvement of skin smoothness, and diminished hyperpigmentation (Fisher, Talwar, Lin, & Voorhees, 1999). Retinoids are also the core of topical therapy for acne because they are comedolytic and anti-inflammatory (Leyden, Stein-Gold, & Weiss, 2017).

ATRA induces skin irritation, hair loss (Foitzik, Spexard, Nakamura, Halsner, & Paus, 2005), and desquamation (Cheong, Lee, & Lee, 2017). Thus, its use in dermatology is strongly limited. ATRA is highly susceptible to photo-degradation due to its conjugated polyene structure. Thus, the use of ATRA carries inherent uncertainty and unreliability (Patwekar, Pedewad, & Gattani, 2018). Retinyl esters readily photodegrade and are more photolabile than retinol (Fu et al., 2007). Even though, the number of cosmetic retail products containing retinyl palmitate (RP)

had increased rapidly (Mei et al., 2005) because of the beneficial effects on the appearance of skin; its genotoxicity upon UVA exposure was reported (Cherng et al., 2005). Thus, the use of ATRA and RP should be avoided in cosmetics and personal care products. To minimize its toxic effects, the stabilization of ATRA was envisioned by designing a polymer conjugate. Particularly, the use of Hyaluronic acid or hyaluronan (HA) is preferred. HA is a biodegradable and biocompatible polymer ubiquitously present in the human body, which consists of D-glucuronic acid (GlcA) and *N*-acetyl-D-glucosamine (GlcNAc) units linked by alternating β-(1→4)-and β-(1→3)- glycosidic bonds. This polysaccharide is a primary structural component of skin extracellular matrix and plays a pivotal role in both fibrotic and regenerative wound healing (Tolg, Telmer, & Turley, 2014). Low molecular weight HA (20–300 kDa) passes through the stratum corneum, so that it can deliver to the deeper layer of the dermis (Nashchekina & Raydan, 2018). The covalent conjugation of HA and ATRA might allow a synergy of the properties of biologically active molecules.

Among the various reactions used for the hydrophobic modification of HA, esterification of either the carboxyl or hydroxyl groups is one of the most studied reactions. HA esters can be prepared by the method described in a previous work (Ventura et al., 2007). However, HA was first converted to its quaternary ammonium salt. The HA-TBA complex can be solubilized in an organic solvent and reacted with the acylation agent. This conversion increases the risk of HA-chain fragmentation. Besides, anhydrous solvents should be regarded as specialty chemicals as they are expensive for an industrial process. A second work deals with the chemical modification of HA mediated by 1-ethyl-3-(3-dimethylaminopropyl) carbodiimide (EDC)/ *N*-hydroxysuccinimide (NHS) in formamide (Yao, Zhang, Zhou, Liu, & Zhang, 2013). However, formamide is a solvent of limited use in pharmaceutical development due to its genotoxicity

(Warheit, Kinney, Carakostas, & Ross, 1989). Similar anhydrous conditions were used for the chemical modification of polyvinyl alcohol (Castleberry, Quadir, Sharkh, Shopsowitz, & Hammond, 2017), pullulan (Lee, Jeong, Seo, & Na, 2013), or Pluronic F127 (Zhu et al., 2019) with retinoids.

In the process of developing biomedical products, the identification of degradation products is imperative when completing the biological evaluation of medical devices under ISO10993. Particularly, ATRA could degrade by light, temperature or oxygen therefore the bioavailability may change.

This work aimed was to extend the mixed anhydrides methodology for chemical modification of HA with antioxidants in water, and to ensure the reproducibility of the reaction. Covalently attached retinoic acid to hyaluronic acid could present different degradation pattern upon UVA exposure than low molecular weight analogs. The structure of the derivatives was elucidated by Nuclear Magnetic Resonance (NMR), UV-Vis, SEC-MALS, and thermogravimetry (TGA). Moreover, the stability of the derivative during aging (up to twelve months) will be discussed.

After the conjugation, the cytotoxicity of ATRA, HA-ATRA, and its low molecular weight analog RP was evaluated. The aim of the study was to explore the effect of a new formulation containing the derivative. HA-ATRA reduced the biomarkers of inflammation interleukin-6 (IL-6), and interleukin-8 (IL-8). The skin penetration of a nanomicellar solution of Nile Red encapsulated in HA-ATRA was assayed using porcine skin model. We also examined the gene expression of HA-ATRA. Thus, the conjugate entered the cells and kept the activity of parent ATRA.

Furthermore, the photoprotective effects of selected antioxidants could further enhance the stability, scavenge the free-radicals and inhibit the photodegradation. To a certain extent, the flavonoid -morin could delay the photo-oxidation of the conjugate, and the complex could present significant free-radical scavenging activity and exhibited excellent long-term stability. Thus, the physical mixture of HA-ATRA/morin would have a wide range of applications for skin delivery.

2. Experimental section

2.1 Materials

Sodium hyaluronate of several Mw (Table 1) was provided by Contipro a.s. (Dolni Dobrouc, Czech Republic) and was characterized before chemical modification. Isopropanol (IPA, 99.7 %), ethanol (99 %) were purchased from Lach-Ner (Czech Republic). Benzoyl chloride (BC, 99%), triethylamine (TEA, 98 %), 4-(dimethylamino) pyridine (DMAP, 99.5%) were bought from Merck. Deuterium oxide (D_2O, 99.8%) was purchased from CortecNet (France). All-trans-retinoic acid (2E,4E,6E,8E)-3,7-dimethyl-9-(2,6,6-trimethylcyclohexen-1-yl) nona-2,4,6,8-tetraenoic acid, 98%, ATRA) was bought from Santiago chemicals a.s (Czech Republic). L-ascorbic acid (99.8%) was bought from Kutilov (Czech Republic). Morin hydrate (2′,3,4′,5,7-pentahydroxyflavone, powder, ≥ 85 %), avobenzone (1-(4-methoxyphenyl)-3-(4-tert-butylphenyl)-1,3-propanedione, 98.5 %), 2-ethylhexyl-2-cyano-3,3-diphenylacrylate 97 %, 2-ethylhexyl 4-methoxycinnamate 98 % (OMC), hydroquinone ≥ 99% (1,4-Benzenediol), (±)-6-hydroxy-2,5,7,8-tetramethylchromane-2-carboxylic acid 97 % (trolox), butylated hydroxytoluene ≥ 99 % (BHT), butylated hydroxyanisole ≥ 98.5 % (BHA), Nile red ≥ 98 %, retinyl palmitate

(Type IV, ~1,800,000 USP units/g, oil), gelatin from porcine skin gel strength 300, Type A, Retinyl acetate ≥ 90 %, retinol, DMEM (Dulbecco's modified Eagles medium-low glucose, glutamine (0.3 mg/mL), glucose (4 mg/mL), penicillin (100 units/mL) with streptomycin (0.1 mg/mL), formic acid ≥ 98 %, and serum were purchased from Sigma-Aldrich. 3-(4,5-dimethylthiazol-2-yl)-2,5-diphenyltetrazolium bromide (MTT, ≥ 98%) and ethidium homodimer suitable for fluorescence, ~90% (HPCE), were purchased from Life Technologies. Anhydrous Acetonitrile (for HPLC) was obtained from VWR chemicals (max. 0.003% H_2O) ≥ 99.95 % CHROMANORM®.

2.2. General procedure for the synthesis of HA-ATRA

Hyaluronic acid (0.5 g, 1.3 mmol of HA dimer) was dissolved in 10 mL of demineralized water. To that solution, IPA (5 mL), TEA (0.35 mL, 2.5 mmol), and DMAP (9 mg, 0.063 mmol were consecutively added. In a second reaction flask, 0.113 g (0.4 mmol) of ATRA was dissolved in IPA (5 mL), followed by TEA (0.35 mL, 2.5 mmol) and benzoyl chloride (0.044 mL, 0.4 mmol) were consecutively added. The equivalents in the reaction were varied as resumed in **Table 1**. The formation of the mixed anhydride was carried out for 60 minutes at 5°C. Then, the mixed anhydride was slowly added to the solution containing HA. The esterification was carried for 3 hours at 5°C. The crude product was isolated by precipitation by addition of 0.35 g of sodium chloride. The product was washed out by addition of 100 mL of IPA and washed with IPA: H_2O (80% v/v, 4 x 100 mL) and finally dried by IPA (2x 100 mL).

2.3. Determination of chemical structure by Nuclear Magnetic Resonance (NMR) Spectroscopy

^{1}H and ^{13}C NMR spectra were carried out at 25°C on a BRUKER Biospin 4G Magnet system 700/54 Ascend operating at a frequency of 700 MHz. The chemical shifts were referenced to 3-(trimethylsilyl)-propionic acid sodium salt (internal standard). HA samples were analysed by dissolving 10 mg of the derivatives in 800 µL of D_2O. 2D HSQC NMR spectra were acquired using edited gradient pulse sequence and 1k data points, 3 kHz spectral width in f2, 80 scans per increment, 256 increments, and heteronuclear scalar coupling C-H set at 145 Hz. DOSY NMR experiments were performed using a stimulated echo pulse sequence with bipolar gradients (2.5 ms) and watergate 3-9-19 pulse train with gradients, diffusion time 0.8 s, and sine-shaped pulses with 32.030 G cm^{-1}. The degree of substitution (DS_{NMR}) is defined as the average number of substituted hydroxyl groups per HA dimer unit and was determined by normalising the integral of the anomeric proton HA signals from 4.6 to 4.3 ppm to 200 (dimers) and reading the integral value corresponding to the methyl moieties of ATRA (**eq. 1**).

$$DSNMR = \frac{I1.7 + I1.6 + I1.4}{3} \qquad \text{Eq. (1)}$$

2.4. Determination of degree of chemical modification by UV-vis spectroscopy

UV/Vis spectroscopy was performed on a Varian CARY 100 UV-Vis Spectrophotometer in the range of 200–800 nm. UV spectra were processed by software UV Probe version 2.00. The hydrolysis of the retinoic ester was carried out for a precise determination of the degree of substitution (DS_A). The amount of free retinoic acid was evaluated by using a calibration curve. The calibration curve was found to be linear in the range of 1 to 10 µg/ mL (**supl. section S1**).

2.5. Thermogravimetric analysis (TGA)

Thermogravimetric measurements were carried out using a TGA Q500 (TA Instruments). 5 mg of sample was heated at a heating rate of 10°C/min under nitrogen atmosphere (up to 600°C) followed by synthetic air atmosphere (up to 910°C). All experiments were carried out in duplicate.

2.6. SEC-MALS

The chromatographic system consisted of an Agilent degasser Model G 1379A, an Agilent HPLC pump Model G 1310A, a Rheodyne manual injector Model 7125i, two 7.8 mm Ultrahydrogel Linear columns (Waters), chromatographic detectors DAWN EOS, ViscoStar differential viscometer and Optilab rEX differential diffractometer connected in series (Wyatt Technology, Santa Barbara, California). Further experimental details are given in supl section S2.

2.7 Long-term stability studies

Stability studies of HA-ATRA were performed using five independent batches after the process was completely optimized (**table 2**). The chemical stability was evaluated by determining the ATRA content in the formulations by UV-vis, HPLC, and NMR (see supplementary section). Samples were packed in 5 g pouches with an inner lining of polyethylene film. Pouches were welded to become airtight and closed to avoid as much as possible the presence of air. Samples were submitted to long term accelerated storage at 40 ± 2 °C/ 75 ±5% of relative humidity (rH)

and in 25 ± 2°C/60± 5 % rH in validated climate chambers (Binder, Germany) according to ICH Q1A(R), guide of industry.

2.8 Photo -stability study

A freshly dissolved HA-ATRA (ATRA c= 25.3 or 100 µg/mL, respectively) was exposed to broadband UVA radiation (320–400 nm). A freshly prepared RP solution (5 mg/mL in IPA) was subjected to the same UVA exposure treatment. A 1,000 W xenon solar UV simulator was used, which is equipped with a dichroic mirror (Arc Lamp Housing, Research, 450-1000 W). The emission spectrum of the UVA lamp was further checked using a portable spectroradiometer, which confirmed the manufacturer's declaration. A filter 20CGA-320 (having stain resistance of 1.0 (SR Class 1.0) under ISO 8424) was used, which allowed a cutoff UV light below 320 nm lower than 1.5% of the total emitted light. Hence, the UV source is essentially UVA (315–400 nm). The lamp was stabilized for 10 min before irradiation. The lamp irradiance was measured using UVA-400 C power meter. Finally, antioxidants were used in the formulations at constant concentration (1 w/w % of HA-ATRA).

2.9 Gas Chromatography -coupled to mass spectrometry (GC-MS) analysis of degradation products

Degradation products were characterized by GC-MS performed on an equipment (7890B, Agilent Technologies) with headspace sampler (7697A, Agilent Technologies), automatic-liquid sampler (7693, Agilent Technologies) and single quadrupole mass spectrometer detector (5977A, Agilent Technologies). LC-MS analysis.

2.10. Determination of free retinoic acid in the samples by HPLC.

The amount of free ATRA in the samples was analysed on a HPLC system Alliance e2695 (Waters) after separation using reverse phase. The mobile phase consisted of a mixture of acetonitrile (ACN) and 0.1% formic acid in water. The mobile phase started at 50% of ACN (column pre-treatment) at a flow rate of 1 mL/min, then changed to 50-95% ACN for 4 min at a flow rate of 1.5 mL/min and a further 5 min at a flow rate of 1.0 mL/min of 95% ACN solution, finally 8 min at 50% of ACN. The detection and identification were performed using a photodiode array detector. All-trans-retinoic acid was monitored at 355 nm. The temperature in the column is 30°C. The values were obtained based on a calibration curve valid in a concentration of 0.45 to 0.55 µg/mL.

2.11 Cell cultivation

NIH-3T3 cells (fibroblasts) were purchased from ATCC (CRL-1658™, Manassas, USA), HaCaT cells from Hölzel diagnostika (Köln, Germany). NIH- 3T3 were cultivated in Dulbecco's modified Eagles medium - low glucose (DMEM) supplemented with 10% FBS, glutamine (0.3 mg/mL), glucose (4 mg/ mL), penicillin (100 units /mL) and streptomycin (0.1 mg/mL) in 5% CO_2 at 37 °C in 75 cm^2 culture flask till the 5^{th} passage. HaCaT were cultivated alike NIH-3T3 without the glucose addition to the medium. Cells were sub-cultured two to three times per week after reaching 80% confluency using 0.25 % trypsin. The cell toxicity of HA-ATRA derivatives was evaluated using fibroblasts (NIH-3T3). The cytotoxicity was compared to the analogous RP and ATRA, which were previously dissolved in isopropanol and DMSO, respectively. Cells were

seeded into 96-well plates and incubated for 24 hours. The cell viability was measured 0, 24, 48, and 72 hours after treatment using the 3-(4, 5-dimethylthiazol-2-yl)-2,5-diphenyl-tetrazolium bromide (MTT) assay. MTT stock solution (20 µL; of concentration 5 mg/mL) was added to the cell culture medium (200 µL) in each well. The plates were incubated for 2.5 h at 37 °C. Then, after removing of the MTT solution, 220 µL of lysis solution was added, and lysis was carried out for 30 min at room temperature, and the optical density was measured by a microplate reader VERSAmax at 570 nm.

2.12. Anti-inflammatory effect of HA-ATRA

The anti-inflammatory properties of HA-ATRA were examined using keratinocytes. HaCaT cells were seeded in a 6-well plate and cultivated for 24 h with HA-ATRA (0.01 % µg/mL). After that, they were irradiated by UVB (dose= 10 mJ/cm^2) and incubated for 22 h. The total RNA was isolated from the samples using RNeasy Mini Kit (Qiagen) according to the instructions provided by the supplier. The concentration and purity of isolated RNA were determined using a NanoDrop OneC Microvolume UV-Vis spectrophotometer using the 260/280 nm absorption ratio. 1 µg of total RNA was used for reverse transcription PCR (RT-qPCR), performed with High Capacity RNA to cDNA Kit (Invitrogen) in GenePro thermal cycler (Bioer Technology) according to the manufacturer's instructions. Subsequent quantitative real-time PCR (qRT-PCR) was performed with TaqMan gene expression assays (IL6 - s00174131-m1, IL8 - Hs00174103-m, Thermofisher) and TaqMan Fast Advanced Mastermix, in a StepOne real-time PCR cycler (Applied Biosystems). Ribosomal protein L13a (RPL13A) was used as a reference gene for analyzing the transcription profile. Student's T-test was used for the statistical analysis. (* $p<0.05$, ** $p<0.01$, *** $p<0.001$).

2.13. Gene expression activity of HA-ATRA

P19 cells were stably transfected with a plasmid with a pRAREβ2 binding site (PMID: 20492758). P19 cells were seeded into 6-well plates (500,000 per well). The wells were preincubated with 0.1 wt.% gelatin for 5 min. The cells were maintained in DMEM enriched with 10 % of serum. ATRA was dissolved in ethanol, RP was dissolved in IPA before dilution into DMEM without serum. HA-ATRA was dissolved directly into DMEM. The cells were treated with either 1 µM ATRA or HA-ATRA corresponding to 1 µM ATRA content or 7.5 µM RP for 6 hours. The luciferase activity was determined according to the manual for the luciferase assay (Luciferase Reporter Gene Assay, high sensitivity; Roche, Basel, Switzerland). After the treatment, the cells were rinsed with PBS, and 100 µl of lysis buffer was added, incubated 15 min at RT, and the cell lysates were scraped. The luciferase activity was measured immediately in 20 µl of a sample with 100 µl luciferase substrate. Luminescence intensity was integrated over 3s in a plate reader (Envision, PerkinElmer, Waltham, USA). Protein concentration was measured with a BCA assay (Pierce; Sigma-Aldrich). Luminescence was normalized to the protein concentration.

2.14. *In vitro* skin penetration of HA-ATRA

NR-loaded micelles of HA-ATRA were prepared by solvent evaporation method (**suppl. s3**). Skin penetration experiments were evaluated in vertical Franz diffusion cells using full-thickness skin from porcine auricles donated by a local slaughterhouse. The receptor was filled with PBS (0.32 mL) and the skin was clasped between donor and receptor and temperate for 20 minutes in 37°C. The donor was filled with 0.5 mL of solutions – the control PBS, 1 mg/mL of

HA-ATRA + NR, and NR in PBS (1 µg/mL) and covered by Parafilm. The penetration was ended after 20 hours when the skin samples was rinsed by PBS, dried and frozen. The microscopic observation (Nikon Eclipse Ti-E, Nikon Corporation) was proceed after the cryosection of samples (10 µm thickness, Leica CM1950, Leica Biosystems). Each sample was prepared in triplicate.

3. Results and discussion.

3.1 Synthesis and characterization of retinoic acid grafted to HA

The activation of the carboxyl moiety in ATRA is the crucial step in the synthesis. The activation can be mediated by 3-[3-(dimethylamino)propyl]-1-ethylcarbodiimide hydrochloride (EDC), but isomerization was prominent with a (13E)/(13Z) isomer ratio of 3:1 (Christensen et al., 2009). Besides, it is necessary to minimize the isomerization of retinoic acid as the *trans* isomer possesses stronger biological activity than the *cis* product (Matsushima et al., 1992). Moreover, N, N'-dicyclohexylcarbodiimide (DCC) is a potent allergen and sensitizer that degrades in water. For the reasons mentioned above, the activation of retinoic acid was mediated via mixed anhydrides (Huerta-Angeles et al., 2014). In this case, the activation reaction is carried out at low temperature (5-10°C). The temperature is crucial for the formation of the intermediate as degradation is avoided (**Fig. s1**). Moreover, short activation time is required (5 to 60 minutes).

In a second step, HA undergoes esterification, mediated by TEA and DMAP in water mixed with isopropanol (1:1), yielding **HA-ATRA** (**Figure 1)**. The mild reaction conditions did not degrade HA backbone, as demonstrated by the determination of average molecular weight (Mw) of the conjugates (**Table S2).** Particularly, HA-ATRA of degree of substitution higher than 3.0 %

have shown an increase of the weight average molecular weight (Mw) due to possible cross-linking.

At least three independent reactions were performed, to ensure the reproducibility. The reaction is working up to 200g scale with identical chemical characteristics, consistent degree of substitution (DS), yield, and purity. The degree of substitution (DS) can be controlled by varying the molar ratio of retinoic acid in the reaction from 3 to 50% to HA dimer. (**Table 1, entries 2-9**). Using higher equivalents in the reaction feed (**Table 1, entry 10**), many resonance peaks were observed in the NMR spectrum due to isomerization or cycloaddition of ATRA, similar to previously reported (Han et al., 2019; Yao et al., 2013). The reaction mediated by mixed anhydrides can be applied for the chemical modification of HA of a broad molecular weight (from 6,000 to 1,396,000 g/mol on Table 1, entries 1 and 11 to 14).

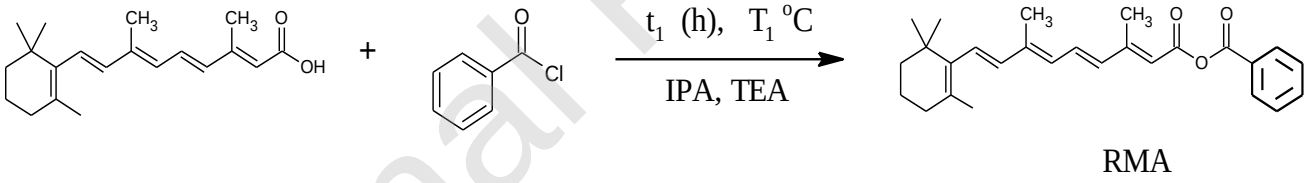

RMA

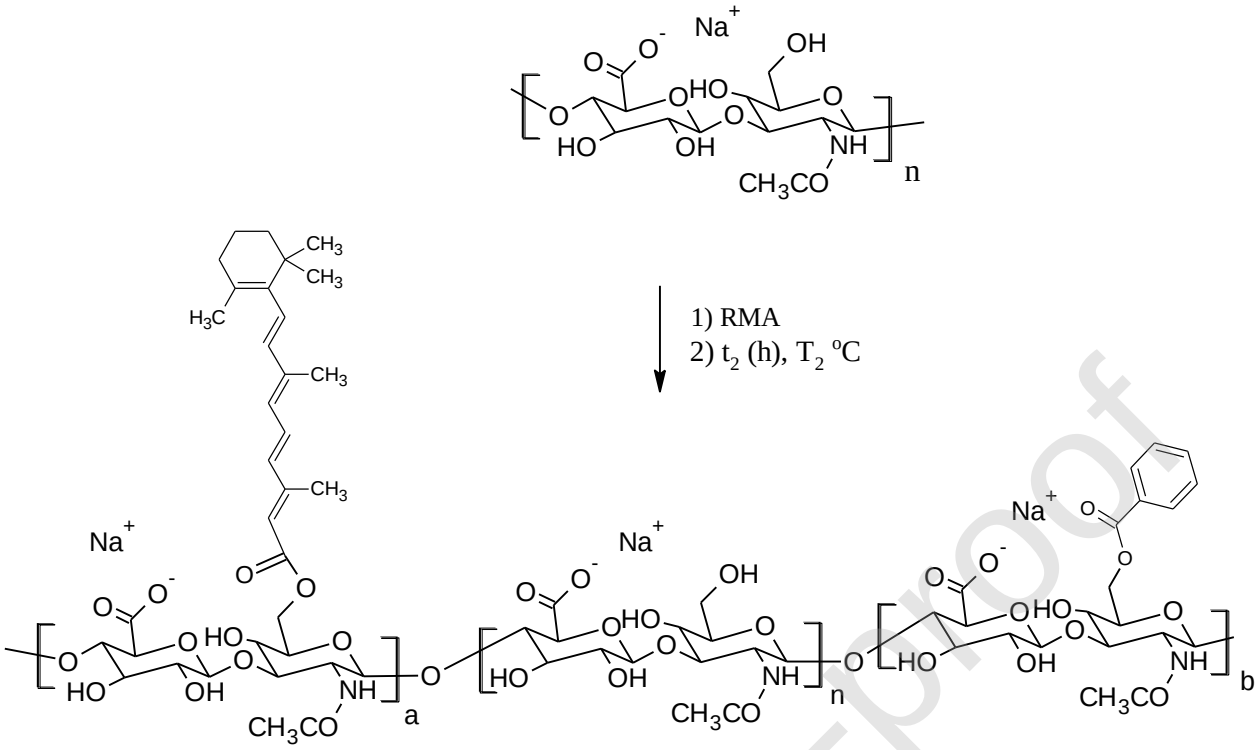

Figure 1. (A)Activation of retinoic acid mediated by benzoyl chloride and (B) esterification of HA by the formed intermediate (RMA). The random distribution of HA modification involves native HA dimers (n); and (b) stands for benzoyl substituents (~2 %) and (a) retinoylation (4% DS) (as an example $DS_A + DS_B = DS_{total}$ = 6%).

3.2 Structural characterization

The chemical structure of the prepared conjugates was confirmed by ^{1}H-NMR (**Fig. 2**). All the spectra showed typical proton chemical shifts of HA involving signal at 2.0 ppm belonging to -$NHCOCH_3$ group, skeletal signals at 3.4–3.9, and anomeric resonances at 4.4–4.6 ppm. Remaining signals detected in the spectrum of modified HA at 0.8, 1.3, 1.6, 2.4; 5.4 and 5.5 ppm, respectively were attributed to CH_3, CH_2, and vinyl functional groups of retinoyl moiety, respectively. Heteronuclear single quantum correlation experiment was used to fully elucidate the

structure of HA-ATRA (**Fig. 3**). The formation of a covalent bond between ATRA and HA was established by diffusion ordered NMR spectroscopy (DOSY). A typical DOSY NMR of retinoylated-HA is shown in **Fig. s2.** The DOSY map demonstrated the absence of free ATRA, which is expected to diffuse much faster than the covalently attached retinoyl moieties.

The purity of the conjugate was confirmed by HPLC after extraction of the free retinoic acid. The amount of the retinoid was detected as lower than 0.035 % wt. Moreover, the purity of the derivatives was tested by thermogravimetry. The conjugate presented values for dry matter (> 85%) and loss of drying (7.0-9.5%), which were reproducible and alike to the values of native HA (**Fig s8b and c**).

HA-ATRA exhibited a strong UV absorption band at λ_{max}= 341 nm. Moreover, a method was developed for the determination of the degree of substitution by UV-vis (see supl. Part **Figs. s3-s7**). Particularly, the determination is useful for low substituted HA-ATRA. The method is based on a calibration curve using retinoic acid as a standard. The degradation of HA-ATRA was reflected as a hypsochromic shifting of the maxima due to loss of conjugation (**Fig. s7**).

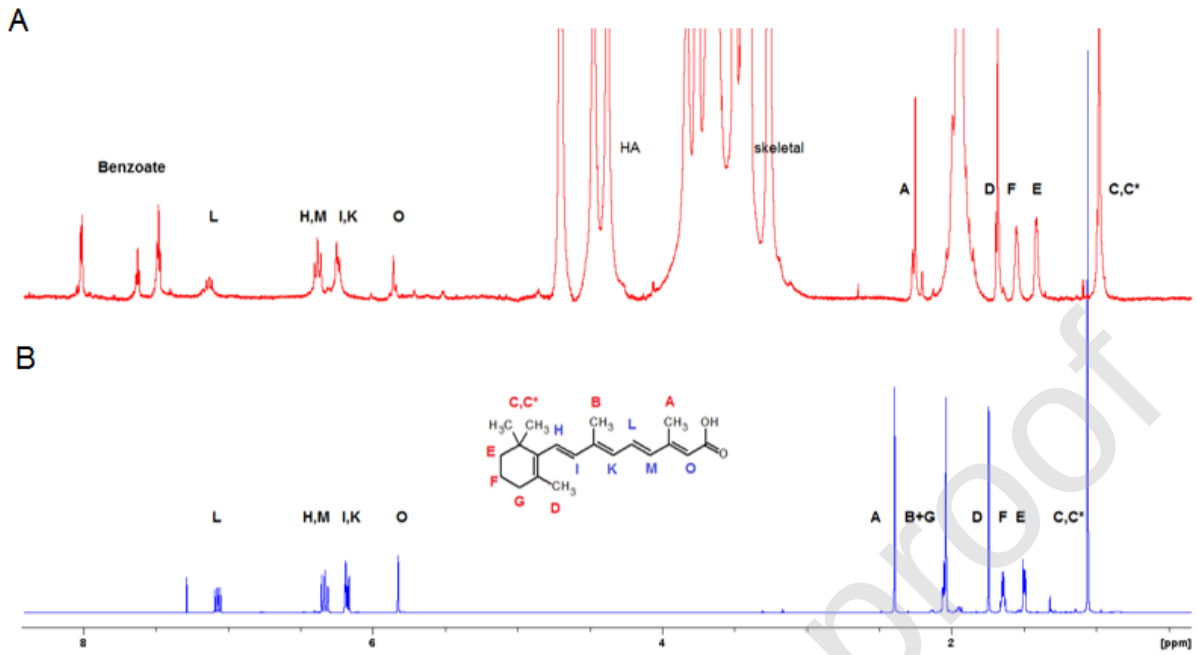

Figure 2. (a) ^{1}H NMR of HA-ATRA conjugate DS= 7.1 % (b) Retinoic acid in $CDCl_3$

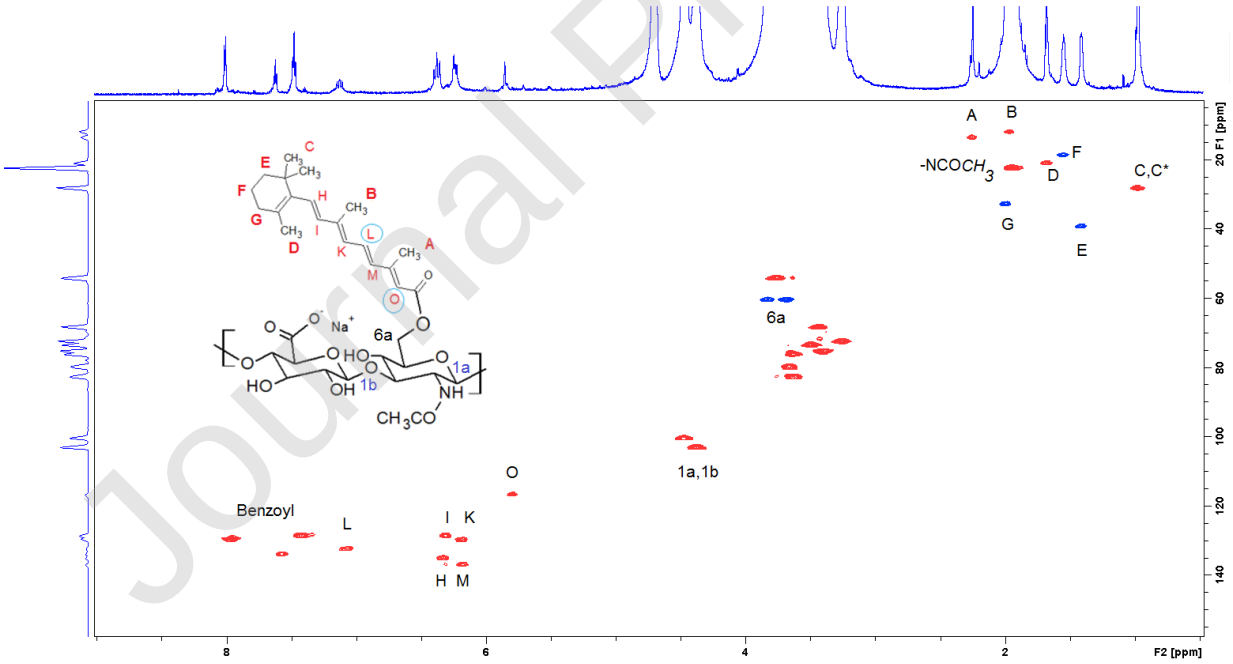

Figure 3. HSQC of HA-ATRA is including the full assignation of the signals.

3.2. Integrity testing of HA-ATRA

After the optimization of the synthetic procedure, stability was followed for three independent batches with degrees of substitution from 0.50, 1.0, 2.0, 3.0 up to 6.0 %.

HA-ATRA was stored at a temperature range of 40 °C ± 2 °C, with humidity set at 75 %RH ± 5 %RH for up to 6 months. This test is referred as "accelerated stability" because high temperature/humidity over a short period of time accelerates product degradation.

Moreover, long term stability storage was tested at 25 °C (± 2) (up to 12 months). The conjugate HA-ATRA remained stable at 25 °C (DS from 0.5 up to 3.0), refrigerated (-5 °C ± 3 °C) or frozen (-15 °C ± 5 °C). Oppositely, drastic changes in the chemical structure and Mw were observed for samples characterized by high DS (**Tables 2, and s2**). Particularly, HA-ATRA degraded fast during accelerated conditions. For evaluating the stability, typical time points are considered 0, 3, and 6-months milestones. The collected data will help advise an expiry date.

Additionally, thermal stability of the conjugate was assessed by thermal gravimetric analysis (TGA). HA-ATRA (DS 2.8 %) and HA (15,000 g/mol) used for chemical modification were compared (**Fig. s8a)**. The thermal degradation of HA could be divided into three stages, namely the moisture evaporation stage (50-150 °C), the devolatilization stage (150-600 °C), and the carbonization stage (600-620 °C). HA-ATRA showed the first step characteristic for water loss up to 100 °C (10 %), followed by a reduction in weight loss at ~200 °C up to 550 °C. The third step is a sharp weight loss characteristic of HA-ATRA degradation at 550 °C. Thus, HA-ATRA showed remarkably lower thermal stability in comparison with HA, which can be explained by the alteration of hydrogen bonding due to the introduction of hydrophobic moieties attached to the polysaccharide backbone. These structural changes represented a more unstable arrangement compared to parent HA (Benešová, Pekař, Lapčík, & Kučerík, 2006). Furthermore, TGA analyses confirmed that the derivative is stable after 6 months of storage (**Fig. s8**).

3.3 Photodegradation kinetics of HA-ATRA and the protective effect of antioxidants

The photostability of the hyaluronan derivative is an essential factor for any application. To investigate whether HA-ATRA can be used for topical and systemic treatments, its photodegradation was followed. Thus, HA-ATRA was irradiated by UVA during various times from 5 seconds up to 60 minutes (section 2.4). Under our experimental conditions, twenty-four minutes of exposure gave a dose of UV radiation of 275 kJ/m^2, i.e. the dose approximately equivalent to ~90 min of sunshine at the French Riviera (Nice) in summer at noon (Damiani et al., 2010).

NMR was used for the qualitative profiling of HA-ATRA, ATRA and RP degradation upon UVA exposure. Additionally, the concentration of HA-ATRA was determined by UV-Vis and expressed as a percentage of their original concentrations using a calibration curve (**supl. s2**). Under the same degradative conditions, both ATRA and HA-ATRA degraded rapidly (**Figs. s9 and s10**). After 30 min upon exposure, 26.8 % of HA-ATRA (DS=5.01 %), and 38.3 % for (DS=2.01 %), have remained.

Oppositely, RP was more stable and kept its chemical structure after 5h of irradiation (**Fig. s11**). However, previous studies dealing with the photodegradation of RP reported that anhydroretinol and 5,6-epoxy-retinyl palmitate were produced upon exposure to UVA radiation (Cherng et al., 2005). These two photodegradation products together with RP itself induced DNA damage and cytotoxicity (Yan et al., 2005). Oppositely, the degradation products of HA-ATRA had proven to be non-cytotoxic (**Fig. s24**).

The major oxidation product upon UVA irradiation was identified as 5,6-epoxy-(E)-retinoic acid (**Fig. s12**). The degradation occurred due to the addition of oxygen radical to the double bond in ATRA (Samokyszyn et al., 2000). The degradation mixture was analyzed by GC-MS (**Fig. s13**). The identification of degradation products allowed us to establish a possible mechanism of degradation. The degradation occurred likely via a mechanism of oxidative breakdown and conversion of 7,8 and 9,10-dioxetanes to secondary degradation products by peroxyl radicals (**Fig. s14).** Thus, 2,6,6-trimethyl-1-cyclohexene-1-carboxaldehyde (β-cyclocitral), β-ionone and (2E,4E)-2-methyl-6-oxohepta-2,4-dienal were identified**.** The last one, it is used for the treatment of several skin conditions. (Burton & Daroszewski, 2006).

To circumvent the fast degradation of HA-ATRA, the synthetic antioxidants (BHT, BHA) were tested. Both antioxidants slowed down the degradation (**Figs. s15 and s16**). However, the

oxidative breakdown of HA-ATRA cannot be entirely avoided. The effect of antioxidants such as: ascorbic acid, histidine, hydroquinone, or trolox was also tested. However, none of them improved the photostability of HA-ATRA as breakdown was always detected (**Figs. s17-s20**).

The photodegradation was followed in the presence of sunscreen agents found commonly in cosmetic formulations (Gonzalez et al., 2007). In the presence of 2-ethylhexyl-4-methoxycinnamate, the degradation of HA-ATRA was similar as of the sample without the stabilizing agent. In the presence of 2-ethylhexyl-2-cyano-3,3-diphenylacrylate, significant photoisomerization was observed after few seconds of irradiation (**Fig s21**). In the presence of avobenzone, the residual amount of the derivative was around 70.5 % after 30 minutes of irradiation.

Finally, morin was found to be the most useful antioxidant as 95% of the conjugate was presented in the mixture (**Fig. 4**). The experimental results demonstrated that morin inhibited the photo-degradation upon 30 min of UVA exposure (**Fig. 4c**). The effect is clearly a function of DS (**Figs 4a and s22**). In agreement of a previous work, the photodegradation of morin was negligible after 30 min of irradiation (**Fig 4b**), (Jangid, Pooja, & Kulhari, 2018). Moreover, morin is an inexpensive flavonoid that presents good bioavailability, therefore, its combination with HA-ATRA becomes a very promising combination for skin.

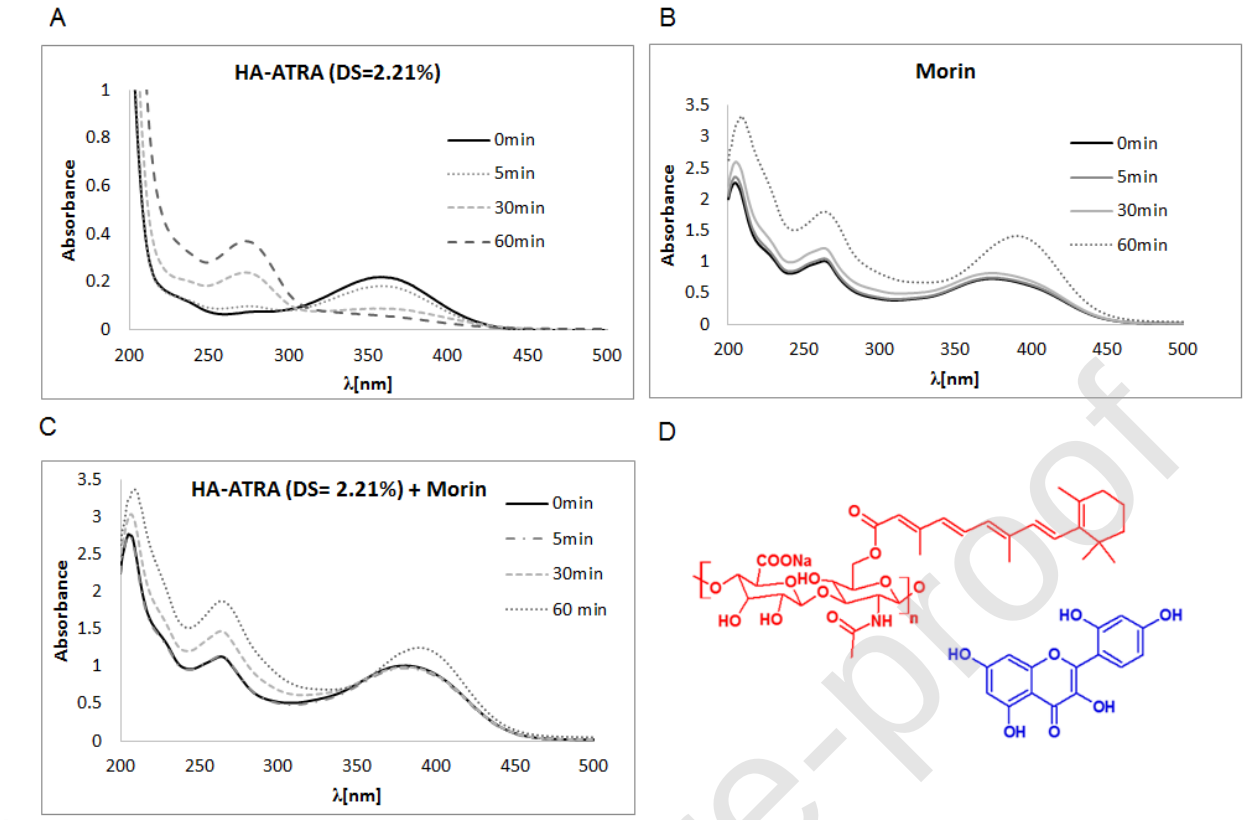

Figure 4. UV-Vis spectra of samples upon UVA irradiation of (a) HA-ATRA (DS = 2.21 %), (b) morin hydrate and (c) HA-ATRA (DS = 2.21 %) + morin hydrate (d) Chemical structure of HA-ATRA and morin.

3.4. Cytocompatibility assay of HA-ATRA

The interaction of cells with modified HA derivatives is essential to be investigated for potential biomedical applications. After chemical modification of HA, its derivatives should not be cytotoxic to healthy cells. Thus, cell proliferation was estimated by MTT metabolic assay. NIH-3T3 fibroblasts were used for determination of non-toxicity. The cytotoxicity of the HA-ATRA (**Table 1, entries 3 and 8**) was assayed and compared with unbound ATRA and RP. The test methods designed to evaluate the acute adverse biological effects of novel compounds is tested after 24h, as described by ISO norm 10993-5: tests for cytotoxicity—*in vitro* methods. The

cytotoxicity was assessed by direct contact assay using as control untreated cells. Moreover, the organic solvents used for the dissolution of the low molecular weight analogues (RP and ATRA) were also included as controls (**Fig. 5)**. After the standard period of incubation of 24 h, the derivatives have not shown any acute cytotoxicity (concentration from 10 to1000 µg/mL). Longer incubation times were also tested to investigate its effect on cytotoxicity. The derivative showed a slightly cytotoxic effect at the highest concentration.

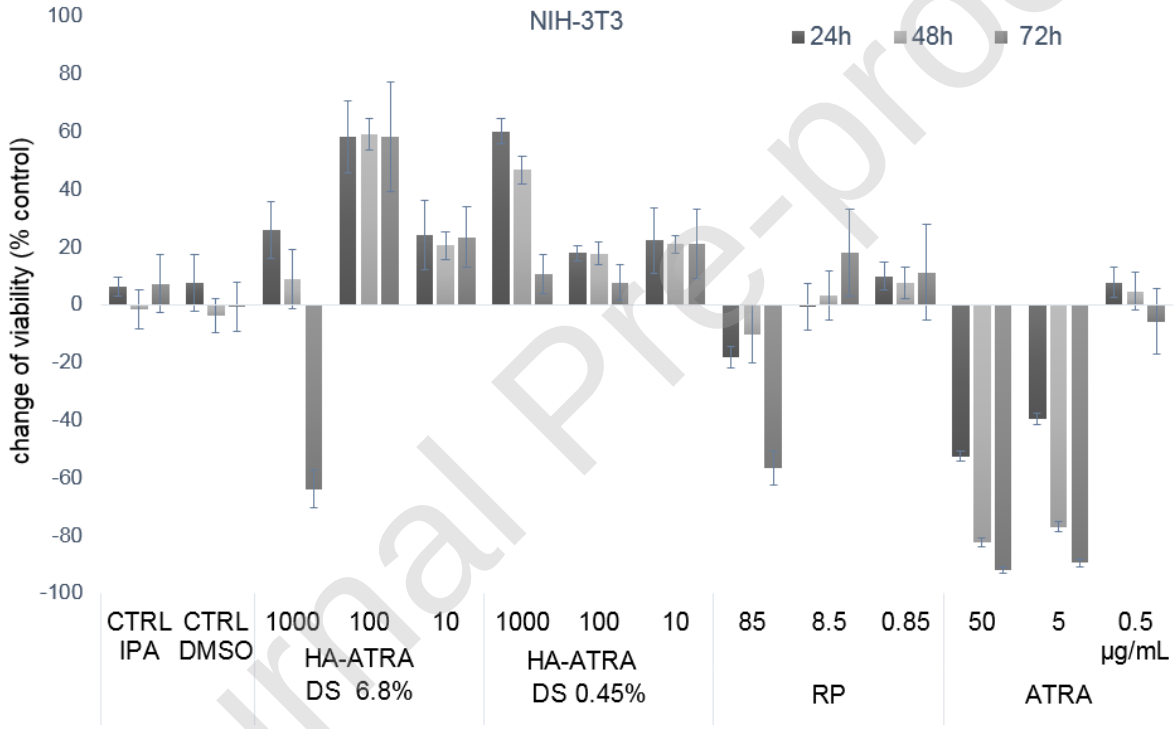

Figure 5. Cell viability of NIH-3T3 fibroblasts in MTT assay after treatment with HA-ATRA (**Table 1, entries 3 and 10**), retinyl Palmitate (RP), and all trans-retinoic acid (ATRA), (mean ± SD, n = 3).

3.5. Anti-inflammatory effect of HA-ATRA in keratinocytes.

Human keratinocytes (HaCaT) were pre-treated with HA-ATRA and exposed under UVB. After 22 h of incubation, total RNA was isolated, and RT-qPCR was performed. The results showed downregulation in gene expression of pro-inflammatory interleukin 6 and 8 (*IL6* and *IL8*) in comparison to the control (non-treated cells). Pro-inflammatory cytokines are presented during inflammation, they include interleukins *IL-1α, IL-1β, IL-6, IL-8, and IL-12* (Schmidt & Gans, 2011). HA-ATRA reduced the biomarkers of inflammation. These results indicated that the cells neutralized the stressful conditions thanks to HA-ATRA effect. Moreover, negligible differences were observed for degree of substitution (0.5 to 2.0 %). The effect was compared with other retinoids commonly used in dermocosmetics (**Figure 6**). HA-ATRA proved to be one of the most efficient retinoids in downregulating interleukins 6 and 8. Oppositely, RP did not show any anti-inflammatory properties.

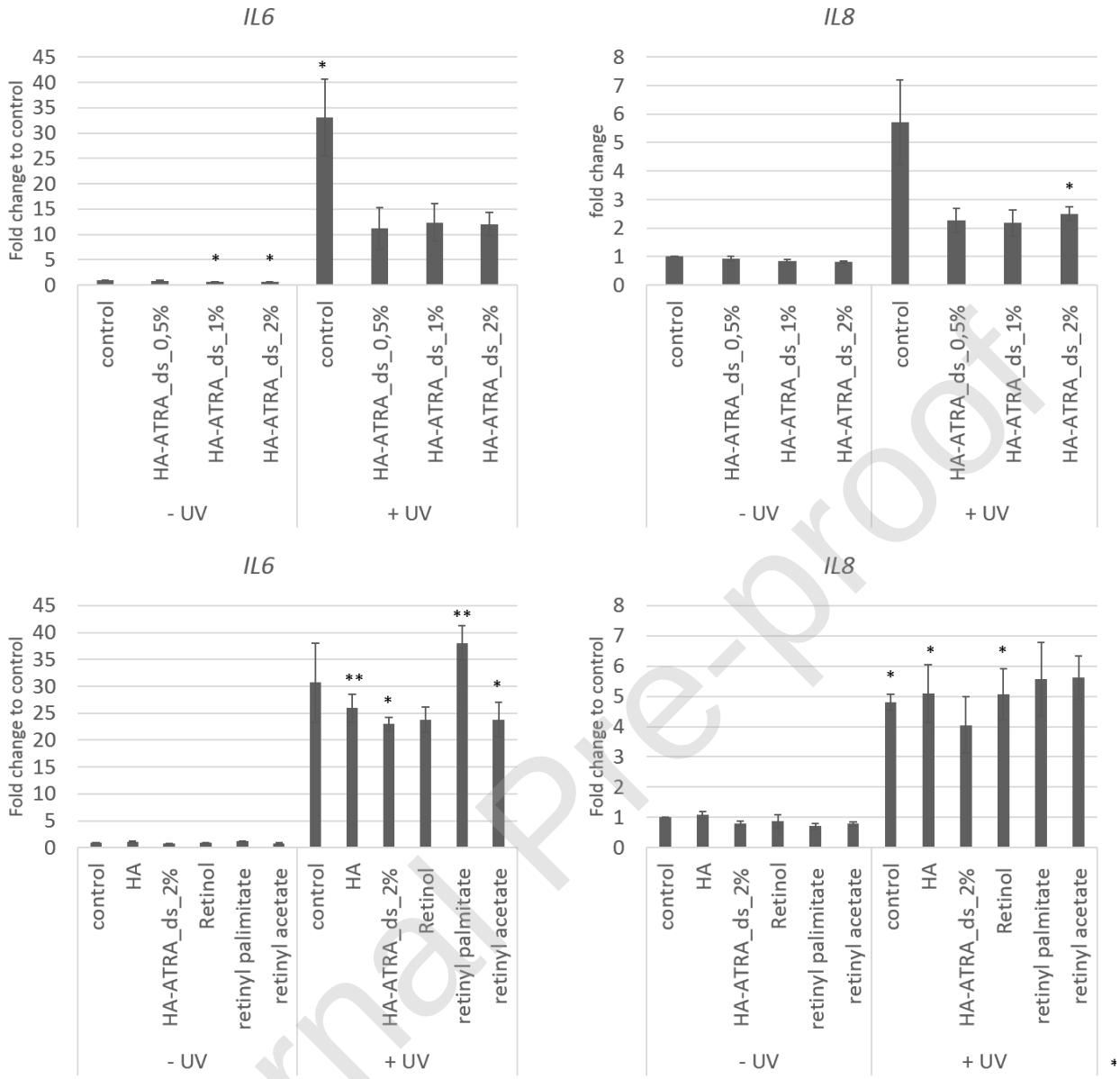

Figure 6. Anti-inflammatory effect of HA-ATRA. The gene expression of *IL6* and *IL8* in irradiated HaCaT keratinocytes was significantly lower after incubation with HA-ATRA (100 µg/mL) in comparison with control (mean ± SD, n = 3).

Furthermore, Nile red (NR) was encapsulated (HA-ATRA+NR) to evaluate the skin penetration of the HA-ATRA derivative. NR was dispersed in PBS served as a control. The

transport of NR was enhanced when encapsulated in HA-ATRA compared to free NR. Specifically, NR was able to reach the lower part of skin and penetrate to the dermis. Oppositely, free NR was localized only in epidermis (**Fig. 7**). Retinol showed the same behaviour (**Fig. s23**).

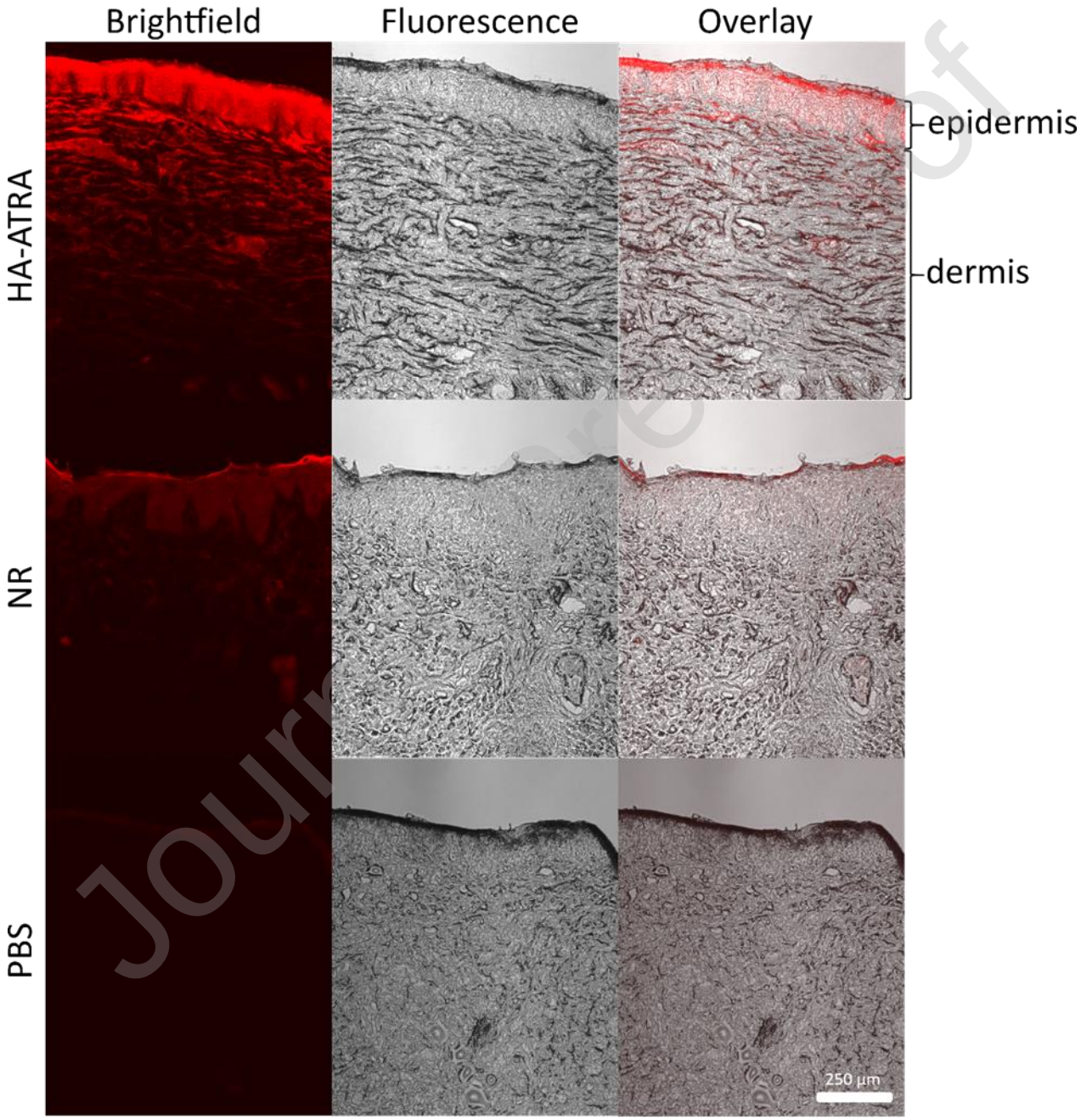

Figure 7. Representative images of the porcine full-profile skin after 24 hours of treatment in Franz-diffusion cells with NR loaded in HA-ATRA, NR dispersed in PBS and PBS (control).

3.6. HA-ATRA activation of canonical ATRA-gene expression

ATRA exerts its biological effects partially by regulation of gene expression. ATRA binds to nuclear receptors, which then bind to retinoic acid response elements (RAREs) and influence gene expression (Al Tanoury, Piskunov, & Rochette-Egly, 2013). We investigated whether ATRA covalently attached to HA could prevent ATRA ability to upregulate gene expression in a luciferase reporter system expressed in cells (**Fig. 8**). This reporter system is triggered by binding of the nuclear receptor and ATRA to a canonical RARE. HA-ATRA increased gene expression showed by an increase of luminescence comparable to that of ATRA. While, RP failed to induce gene expression of luciferase in the reporter system. Thus, RP needs to be metabolized to ATRA to exhibit its genomic effects. Moreover, RP may have limited availability in cells because of its high hydrophobicity and low solubility in water. The results highlighted that HA-ATRA can enter cells and keep the activity of ATRA.

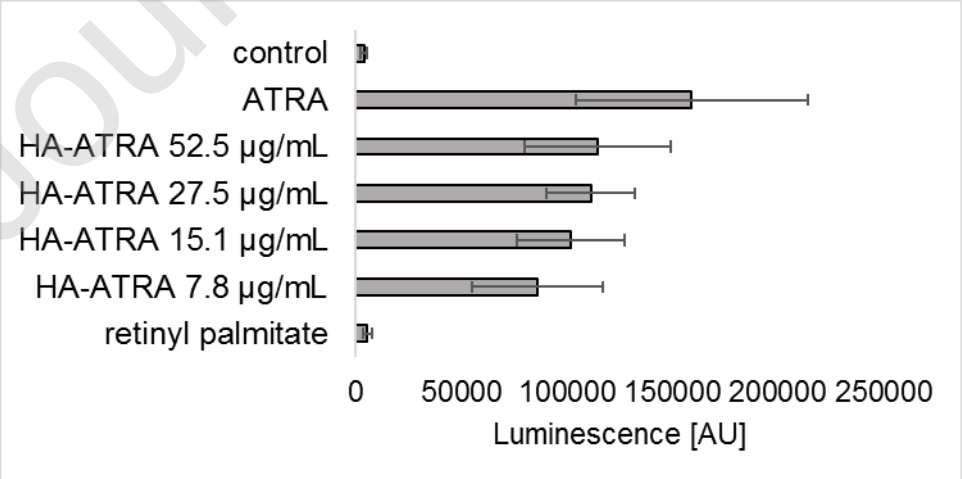

Figure 8. Induction of gene expression by HA-ATRA. The activity of ATRA or its derivates was assessed *in vitro* cellular luciferase reporter assay. P19 cells were treated with 1 µM ATRA, HA-ATRA corresponding to 1 µM content of ATRA or 7.5 µM RP. Activation of luciferase gene expression leads to increase in luminescence (mean ± SD, n = 4).

4. Conclusions

Here, we reported the chemical characterization of a water-soluble derivative of HA and retinoic acid, which was obtained via mixed anhydrides. The conjugation of HA and ATRA improved the shelf-life stability of the conjugate. The chemical stability is a clear function of the degree of chemical modification of the polysaccharide.

The results of the evaluations on the photoprotective effects on antioxidants on photodegradation showed that the protective effects of antioxidants are minimal. We have demonstrated that morin is an effective antioxidant. The presence of (0.1 % wt) of morin lead to photostabilization. We conclude that HA-ATRA is physico-chemically more labile to photolysis than retinyl palmitate. Furthermore, the photodegradation of HA-ATRA produced: β-cyclocitral, β-ionone, 5,6-epoxy-(E)-retinoic acid and follows a breakdown mechanism. The photodegradation of HA-ATRA had not produced toxic products. No significant differences in cell viability were observed after 24 and 48 h indicating a good cytocompatibility.

Furthermore, HA-ATRA was able to downregulate the expression of pro-inflammatory cytokines (*IL-6, IL-8*). Topical application of HA-ATRA represent a good approach to deliver directly to the dermis; which could be used for drugs or cosmeceuticals. Thus, HA-ATRA is of pivotal interest in wound healing, anti-aging, and pharmaceutics.

Acknowledgements

The study was supported by funds of the European Regional Development Fund - Project INBIO (No. CZ.02.1.01/0.0/0.0/16_026/0008451). The authors wish to thank Jaroslav Novotný for the determination of thermal properties, Lenka Hejlová for the determination of SEC-MALLS and Tereza Hanová for the optimization of the HPLC method.

References

Al Tanoury, Z., Piskunov, A., & Rochette-Egly, C. (2013). Vitamin A and retinoid signaling: genomic and nongenomic effects. *J Lipid Res, 54*(7), 1761-1775.

Benešová, K., Pekař, M, Lapčík, L, & Kučerík, J. (2006). Stability evaluation of n-alkyl hyaluronic acid derivates by DSC and TG measurement. *J Therm Anal Calorim, 83*(2), 341-348.

Burton G. William, Daroszewski Janusz. (2006). Topical formulations for the treatment of skin conditions. *EP1727530, A2*.

Castleberry, S. A., Quadir, M. A., Sharkh, M. A., Shopsowitz, K. E., & Hammond, P. T. (2017). Polymer conjugated retinoids for controlled transdermal delivery. *J Control Release, 262*, 1-9.

Cheong, Kyung Ah, Lee, Tae Ryong, & Lee, Ai-Young. (2017). Complementary effect of hydroquinone and retinoic acid on corneocyte desquamation with their combination use. *Journal of Dermatological Science, 87*(2), 192-200.

Cherng, S. H., Xia, Q., Blankenship, L. R., Freeman, J. P., Wamer, W. G., Howard, P. C., & Fu, P. P. (2005). Photodecomposition of retinyl palmitate in ethanol by UVA light-formation of photodecomposition products, reactive oxygen species, and lipid peroxides. *Chem Res Toxicol, 18*(2), 129-138.

Christensen , S., Pedersen , J., Andresen, L., Madsen, Robert, & Clausen , H. (2009). Isomerization of all-(E)-Retinoic Acid Mediated by Carbodiimide Activation – Synthesis of ATRA Ether Lipid Conjugates. *Eur J Org Chem, 2010*(4), 719-724.

Damiani, Elisabetta, Astolfi, Paola, Giesinger, Jochen, Ehlis, Thomas, Herzog, Bernd, Greci, Lucedio, & Baschong, Werner. (2010). Assessment of the photo-degradation of UV-filters and radical-induced peroxidation in cosmetic sunscreen formulations. *Free Radical Research, 44*(3), 304-312.

Essendoubi, M., Gobinet, C., Reynaud, R., Angiboust, J. F., Manfait, M., & Piot, O. (2016). Human skin penetration of hyaluronic acid of different molecular weights as probed by Raman spectroscopy. *Skin Res Technol, 22*(1), 55-62.

Fisher, G. J., Talwar, H. S., Lin, J., & Voorhees, J. J. (1999). Molecular mechanisms of photoaging in human skin in vivo and their prevention by all-trans retinoic acid. *Photochem Photobiol, 69*(2), 154-157.

Foitzik, K., Spexard, T., Nakamura, M., Halsner, U., & Paus, R. (2005). Towards dissecting the pathogenesis of retinoid-induced hair loss: all-trans retinoic acid induces premature hair follicle regression (catagen) by upregulation of transforming growth factor-beta2 in the dermal papilla. *J Invest Dermatol, 124*(6), 1119-1126.

Fu, Peter P., Xia, Qingsu, Yin, Jun Jie, Cherng, Shu-Hui, Yan, Jian, Mei, Nan, . . . Wamer, Wayne G. (2007). Photodecomposition of Vitamin A and Photobiological Implications for the Skin. *Photochemistry and Photobiology, 83*(2), 409-424.

Gonzalez, H., Tarras-Wahlberg, N., Strömdahl, B., Juzeniene, A., Moan, J., Larkö, O., . . . Wennberg, A. M. (2007). Photostability of commercial sunscreens upon sun exposure and irradiation by ultraviolet lamps. *BMC Dermatol, 7*, 1.

Han, Lingfei, Hu, Lejian, Liu, Fulei, Wang, Xin, Huang, Xiaoxian, Liu, Bowen, . . . Qu, Wei. (2019). Redox-sensitive micelles for targeted intracellular delivery and combination chemotherapy of paclitaxel and all-trans-retinoid acid. *Asian Journal of Pharmaceutical Sciences, 14*(5), 531-542.

Huerta-Angeles, Gloria, Bobek, Martin, Přikopová, Eva, Šmejkalová, Daniela, & Velebný, Vladimír. (2014). Novel synthetic method for the preparation of amphiphilic hyaluronan by means of aliphatic aromatic anhydrides. *Carbohydrate Polymers, 111*, 883-891.

Jangid, Ashok Kumar, Pooja, Deep, & Kulhari, Hitesh. (2018). Determination of solubility, stability and degradation kinetics of morin hydrate in physiological solutions. *RSC Advances, 8*(50), 28836-28842.

Lee, Jieun, Jeong, Dooyong, Seo, Seogjin, & Na, Kun. (2013). Biodegradable nanogel based on all-trans retinoic acid/pullulan conjugate for anti-cancer drug delivery. *Journal of Pharmaceutical Investigation, 43*(1), 63-69.

Leyden, J., Stein-Gold, L., & Weiss, J. (2017). Why Topical Retinoids Are Mainstay of Therapy for Acne. *Dermatol Ther (Heidelb), 7*(3), 293-304.

Matsushima, Youko, Kawachi, Emiko, Tanaka, Hideo, Kagechika, Hiroyuki, Hashimoto, Yuichi, & Shudo, Koichi. (1992). Differentiation-inducing activity of retinoic acid isomers and

their oxidized analogs on human promyelocytic leukemia HL-60 cells. *Biochemical and Biophysical Research Communications, 189*(2), 1136-1142.

Mei, N., Xia, Q., Chen, L., Moore, M. M., Fu, P. P., & Chen, T. (2005). Photomutagenicity of retinyl palmitate by ultraviolet a irradiation in mouse lymphoma cells. *Toxicol Sci, 88*(1), 142-149.

Nashchekina, Yu. A., & Raydan, M. (2018). Noninvasive penetration of 5 nm hyaluronic acid molecules across the epidermal barrier (in vitro) and its interaction with human skin cells. *Skin Research and Technology, 24*(1), 129-134.

Patwekar, S. L., Pedewad, S. R., & Gattani, S. (2018). Development and evaluation of nanostructured lipid carriers-based gel of isotretinoin. *Particulate Science and Technology, 36*(7), 832-843.

Samokyszyn, V. M., Gall, W. E., Zawada, G., Freyaldenhoven, M. A., Chen, G., Mackenzie, P. I., . . . Radominska-Pandya, A. (2000). 4-hydroxyretinoic acid, a novel substrate for human liver microsomal UDP-glucuronosyltransferase(s) and recombinant UGT2B7. *J Biol Chem, 275*(10), 6908-6914.

Schmidt, N., & Gans, E. H. (2011). Tretinoin: A Review of Its Anti-inflammatory Properties in the Treatment of Acne. *J Clin Aesthet Dermatol, 4*(11), 22-29.

Son, S. U., Lim, J. W., Kang, T., Jung, J., & Lim, E. K. (2017). Hyaluronan-Based Nanohydrogels as Effective Carriers for Transdermal Delivery of Lipophilic Agents: Towards Transdermal Drug Administration in Neurological Disorders. *Nanomaterials (Basel), 7*(12).

Tolg, C., Telmer, P., & Turley, E. (2014). Specific sizes of hyaluronan oligosaccharides stimulate fibroblast migration and excisional wound repair. *PLoS One, 9*(2), e88479.

Ventura, C., Cantoni, S., Bianchi, F., Lionetti, V., Cavallini, C., Scarlata, I., . . . Perbellini, A. (2007). Hyaluronan mixed esters of butyric and retinoic Acid drive cardiac and endothelial fate in term placenta human mesenchymal stem cells and enhance cardiac repair in infarcted rat hearts. *J Biol Chem, 282*(19), 14243-14252.

Warheit, David B., Kinney, Laura A., Carakostas, Michael C., & Ross, Paul E. (1989). Inhalation toxicity study of formamide in rats. *Fundamental and Applied Toxicology, 13*(4), 702-713.

Xie, Jiesi, Ji, Yujie, Xue, Wei, Ma, Dong, & Hu, Yunfeng. (2018). Hyaluronic acid-containing ethosomes as a potential carrier for transdermal drug delivery. *Colloids and Surfaces B: Biointerfaces, 172*, 323-329.

Yan, J., Xia, Q., Cherng, S. H., Wamer, W. G., Howard, P. C., Yu, H., & Fu, P. P. (2005). Photo-induced DNA damage and photocytotoxicity of retinyl palmitate and its photodecomposition products. *Toxicol Ind Health, 21*(7-8), 167-175.

Yao, Jing, Zhang, Li, Zhou, Jianping, Liu, Hongpan, & Zhang, Qiang. (2013). Efficient Simultaneous Tumor Targeting Delivery of All-Trans Retinoid Acid and Paclitaxel Based on Hyaluronic Acid-Based Multifunctional Nanocarrier. *Molecular Pharmaceutics, 10*(3), 1080-1091.

Zhang, S., & Duan, E. (2018). Fighting against Skin Aging: The Way from Bench to Bedside. *Cell Transplant, 27*(5), 729-738.

Zhu, Yan-Hua, Ye, Ning, Tang, Xin-Feng, Khan, Malik Ihsanullah, Liu, Hong-Liang, Shi, Ning, & Hang, Li-Feng. (2019). Synergistic Effect of Retinoic Acid Polymeric Micelles and Prodrug for the Pharmacodynamic Evaluation of Tumor Suppression. *Front in Pharmacol, 10* (447).

Table 1. Optimization of reaction parameters for the preparation of *trans*-retinoic acid grafted to hyaluronan (HA-ATRA).

Entry	M_w[1] HA (kDa)[a]	Eq. RMA/HA[b] (%)	DS_A[c] (%)	DS_A[d]	DS_B[e]	Concentration of retinoic acid (μg/mL)[f]	Yield (%)
1	6.2(1.8)	0.35	6.9	5.2	3.6	8.7	85.0
2	15.0(1.5)	0.03	0.43±0.08	0.7±0.10	0.3	5.4	93.0
3		0.06	1.02±0.06	1.11±0.04	0.6	12.9	95.7
4		0.10	2.05±0.15	2.1±0.10	1.1	25.3	95.6
5		0.15	3.08±0.20	3.1±0.20	2.0	38.5	94.0
6		0.30	4.05±0.25	4.4±0.8	3.6	52.4	96.3
7		0.35	5.60±0.20	6.0±0.45	4.1	87.0	95.0
8		0.50	6.80±0.55	7.10±0.1	4.5	103.7	95.2
9	97(1.6)	0.03	0.32±0.07	0.51±0.06	nd	5.2	79.2
10		0.15	3.30±0.20	3.17±0.21	1.5	35.5	86.0
11		0.30	4.84±0.60	3.56±0.2	4.6	44.2	86.6
12	240(1.6)	0.15	2.0±0.1	3.95±0.4	nd	26.1	86.4
13	470(1.7)	0.15	0.27	0.51	nd	3.4	80.0
14	1396 (1.5)	0.15	0.59	nd	nd	7.3	81.0

[a]The molecular weight of native hyaluronan used for the chemical modification. The polydispersity (PDI=Mw/Mn) is included in brackets.

[b]The activation was carried out for 30 min. at 5°C in THF. The mixed anhydride reacts with HA for 1h at 5°C. All the reactions were performed using 2.5 % (w/v) concentration. At least three independent batches were prepared to ensure the reproducibility of the reaction. Nd means that the measurement was imprecise due to the high viscosity of the sample or low DS.

[c]The degree of substitution for the retinoylated product was determined by UV vis (DS_A) using the calibration curve provided in supl. S1.

[d]the degree of substitution of retinoylated product determined by NMR.

[e] The degree of substitution of benzoylated HA was determined by NMR.

[f]The concentration of retinoic acid after hydrolysis of the polymer was determined by UV Vis.

Table 2. Integrity testing for HA-ATRA evaluated at several time points, stored under defined conditions.

	Time					
Months	**0[a]**	**1**	**2**	**3**	**6**	**12**
Zone II (25 °C±2 °C)	0.50±0.07	0.45±0.08	0.44±0.08	0.45±0.07	0.45±0.05	0.43±0.05
	1.07±0.02	1.10±0.02	1.06±0.03	1.05±0.01	1.07±0.04	0.94±0.04
	1.97±0.04	1.97±0.04	1.92±0.03	2.04±0.08	1.91±0.04	1.74±0.08
	2.96±0.04	2.70±0.09	2.71±0.05	2.68±0.07	2.69±0.08	2.19±0.21[c]
	5.57±0.25	4.35±0.33[c]	2.16±0.26[c]	1.53±0.10[c]	--[b]	--[b]
Refrigerated (-5 °C±3 °C)	5.57±0.25	4.36±0.39[c]	3.53±0.38[c]	2.57±0.18[c]	--[b]	--[b]
Frozen (-15 °C±5 °C)	5.57±0.25	4.35±0.33[c]	4.32±0.51[c]	4.07±0.35[c]	3.64±0.37[c]	3.35±0.34[c]
Accelerated	0.52±0.08	0.48±0.04	0.38±0.06	0.35±0.06	0.32±0.05[c]	--[b]

(40 °C±2 °C)	3.00±0.18	1.97±0.36[c]	1.82±0.57[c]	1.43±0.47[c]	1.05±0.28[c]	--[b]

[a]The degree of substitution was determined by UV-Vis. Each value represents the mean ± standard deviation (n=3). The amount of free retinoic acid in the samples was determined HPLC.

[b]The absorbance was shifted due to degradation.

[c]The sample was considered as non-stable (HA-ATRA ≤ 80 %).